Macromolecular Research, Vol. 14, No. 6, pp 646-653 (2006)

Surface Modification of Magnetites Using Maltotrionic Acid and Folic Acid for Molecular Imaging

K. M. Kamruzzaman Selim, Joo-Hee Lee, Sun-Jung Kim, Zhicai Xing, and Inn-Kyu Kang*

Dept. of Polymer Science, Kyungpook National University, Daegu 702-701, Korea

Yongmin Chang

Dept. of Diagnostic Radiology, Kyungpook National University, Daegu 700-422, Korea

Haiqing Guo

College of Chemistry and Molecular Eng., Peking University, Beijing 100871, China

Received September 14, 2006; Revised October 27, 2006

Abstract: Highly hydrophilic, uniform, superparamagnetic and nontoxic maltotrionic acid (MA)-coated magnetite nano-particles (MAM) were prepared and characterized by TEM, DLS, XRD and VSM. MA was used to improve the biocompatibility, monodispersity and non-specific intracellular uptake of nanoparticles. Folic acid (FA) was subsequently conjugated to the MAM to preferentially target KB cells (cancer cells) that have folate receptors expressed on their surfaces and to facilitate nanoparticles in their transit across the cell membrane. Finally, fluorescence isothiocyanate (FITC) was added to the nanoparticles to visualize the nanoparticle internalization into KB cells. After the cells were cultured in a media containing the MAM and MAM-folate conjugate (FAMAM), the results of fluorescence and confocal microscopy showed that both types of nanoparticles were internalized into the cells. Nevertheless, the amount of FAMAM uptake was higher than that of MAM. This result indicated that nanoparticles modified with MA and FA could be used to facilitate the nanoparticle uptake to specific KB cells (cancer cells) for molecular imaging.

Keywords: magnetite nanoparticles, maltotrionic acid, folic acid, intracellular uptake, particle internalization.

Introduction

Over the past decade, numerous biomedical applications have emerged for superparamagnetic iron oxide nanoparticles dispersed in an aquous medium.[1,2] The combinations of the nanometer size with superparamagnetic properties led to their use in labeling and sorting cells,[3] magnetic resonance imaging (MRI),[4] targeted drug delivery[5]and hyperthermia.[6,7] The addition of fluorescence properties to these magnetic nanoparticles offers new potential for *in vitro* and *in vivo* imaging.[8] But most of these potential applications require magnetic nanoparticles to be thermally and chemically stable, water soluble, biocompitable, biodegradable, nontoxic in physiological medium, small less than 20 nm with overall narrow particles size distribution, highly specific, efficiently and rapidly internalized into specific target cells.[9,10] Due to hydrophobic surfaces and large surface area to volume ratio, *in vivo* use of magnetite nanoparticles is tend to agglomerate and the particles are quickly cleared by macrophages before they can reach target cells. Avoidance of this obstacle is possible if the surfaces of these magnetite nanoparticles are made sufficiently hydrophilic by modifying the surfaces using appropriate biocompatible-polymer and suitable targeting agents. These sorts of modifications are crucial factors that not only determine the biocompatibility of these magnetic materials but also play an important role in cell adhesion on biomaterials.[11,12] To date, a wide variety of coating materials such as dextran, starch, albumin, silicons and poly (ethylene glycol) have been used to prevent aggregation in liquid, to improve chemical stability, to reduce nonspecific protein adsorption and clearance by macrophages and render the nanoparticles capable of crossing the cell membrane.[13,14] But to the best of our knowledge no report has yet been published using maltotrionic acid (MA) as coating material of the magnetite nanoparticles to improve dispersing stability in aqueous medium or blood.

MA is synthesized from maltotriose which is a trisaccharide that consists of three alpha-linked glucose molecules and it

*Corresponding Author. E-mail: ikkang@knu.ac.kr

is the second most abundant sugar in wort (15-20%). It is obtained by enzymic hydrolysis of starch.[15] This is widely used because of low molecular weight (Mw. 520.45) and easy digestion and absorption by body. It has many significant biological advantages such as being biodegradable, biocompatible and bioactive. Its chemical properties include being poly-cationic, hydrophilic and containing polyhydroxy groups.[16,17] On the other hand, to achieve specific cancer cell recognition and high efficiency of nanoparticle intracellular uptake via receptor-mediated endocytosis, a low molecular weight targeting agent such as folic acid (FA) has been coated on the surface of the nanoparticles because it can couple to the folate receptors overexpressed on cancer cell membranes.[18] The folate receptor is not only a tumor marker but also has been shown to efficiently internalize folate molecules to the cell membrane. Furthermore, FA itself is stable and generally poorly immunogenic.[12]

So introduction of maltotrionic acid-folic acid (MA-FA) conjugate to the surfaces of the magnetite nanoparticles through chemical bonding gives the combined advantage of MA and FA. Introduction of MA to the nanoparticle surfaces prevents the nanoparticles from unwanted agglomeration, makes them more biocompatible and increases their non-specific intracellular uptake. On the contrary, FA is grafted onto the distal end of MA chain to target cancer cells specifically. As MA and FA play different role in intracellular uptake of nanoparticles, it is expected that the uptake efficiency will be further improved after the MA-FA conjugate are attached to the nanoparticles surfaces. Despite the well known ability of folate receptor to facilitate internalization of polymeric particles, little effort has been made on delivery of magnetic nanoparticles modified with MA and FA into cells.

In this study, firstly MA-coated magnetite nanoparticles (MAM) were synthesized and their crystallinity, magnetic property, size and shape of the magnetite nanoparticles were determined by X-ray diffractometer (XRD), vibrating sample magnetometer (VSM), transmission electron microscopy (TEM) and dynamic light scattering (DLS), respectively. Then FA was immobilized on the surface of MAM to improve their cell internalization and to target breast cancer cells. The uptake of MA-FA conjugated nanoparticles (FAMAM) into cancer cells (KB cells) was studied using MAM as a control. Fourier transform infrared (FTIR) spectra were used to characterize the immobilization of MA and FA on the nanoparticle surfaces. Finally, fluorescence and confocal microscopy were used to visualize the uptake and track the distribution of the magnetite nanoparticles into the cells.

Experimental

Materials. Ferric chloride hexahydrate ($FeCl_3 \cdot 6H_2O$ > 98%) and ferrous chloride tetrahydrate ($FeCl_2 \cdot 4H_2O$ > 99%), folic acid (FA, $C_{19}H_{19}N_7O_6$ > 98%) were purchased from Sigma Co. (USA). Maltotriose ($C_{18}H_{32}O_6$ > 95%), dialysis tube (Benzoylated, MWCO = 12,000) and other chemicals were purchased from Aldrich Chemical Co. (USA). KB cells and RPMI-1640 medium were purchased from American Type Culture Collection (ATCC, TIB-186, Rock ville, MD). All reagents were analytical grade and were used as received.

Synthesis of Magnetite Nanoparticles. Magnetic nanoparticles of approximately 7 nm diameter were precipitated in alkali solution from the solution of Fe(II) and Fe(III) chloride according to the standard co-precipitation technique of Dresco *et al.*[19] Shortly, the ferric and ferrous chlorides (molar ratio 2 : 1) were dissolved in deoxygenated water at a concentration of 0.1 M of iron ions. The solution was used immediately after preparation. Chemical precipitation was achieved by using a 1 M deoxygenated solution of ammonium hydroxide. The reaction was carried out at 80 °C under vigorous stirring and N_2 ambient environment. The final pH of the solution was maintained between 11 and 12. The magnetite solutions was then dialysed against distilled water until obtaining pH 7.

Synthesis of Maltotrionic Acid. Maltotriose (5 g, 9.92 mmol) was dissolved in hot water (3.8 mL) and diluted with methanol (10 mL). The solution was then mixed with iodine solution prepared by dissolving iodine (5.033 g, 18.83 mmol) in methanol (75 mL). To the mixed solution, 4 wt% of potassium hydroxide methanol solution (175 mL) was added until the iodine color disappeared. The solution was then recrystallized using a methanolic aqueous solution (methanol : water = 12 : 5, 600 mL) to obtain potassium maltotrionate. The resulting potassium maltotrionates were dissolved in distilled water and subsequently passed through an amberlite IR-120 column to obtain maltotrionic acid (MA) (Figure 1).[20]

Surface Modification.

Modification of Magnetite with Aminosilane: The surface of magnetite particles was coated with (3-aminopropyl) triethoxysilane (APTES) by a silanization reaction in order to obtain silane-modified magnetite particles (AM). Briefly, 50 mL of 5 wt% magnetite suspension and 10 mL of APTES aqueous solution were sonicated for 30 min. Acetic acid was added to the solution to adjust pH 4.5~5. The mixture was then heated at 100 °C by silicon oil for 2 h with vigorous stirring. The reaction was carried out under N_2 ambient environment. The silanized suspension was then dialyzed against distilled water for 2 days. After separation by magnet, the silane-coated magnetite particles (AM) were dried into powder at room temperature under vacuum.

Modification of AM with MA: Maltotrionic acid (MA, 0.032 g, 9.2×10^{-4} M) was dissolved in 100 mL phosphate buffer (pH7) containing 1-ethyl-3-(3-dimethylaminopropyl) carbodiimide (EDC) and incubated for 2 h. This solution was then mixed with 1 g of aminosilane coated magnetite and stirred for 48 h at room temperature. The reaction solution was dialyzed for 2 days using sodium bicarbonate buffer to

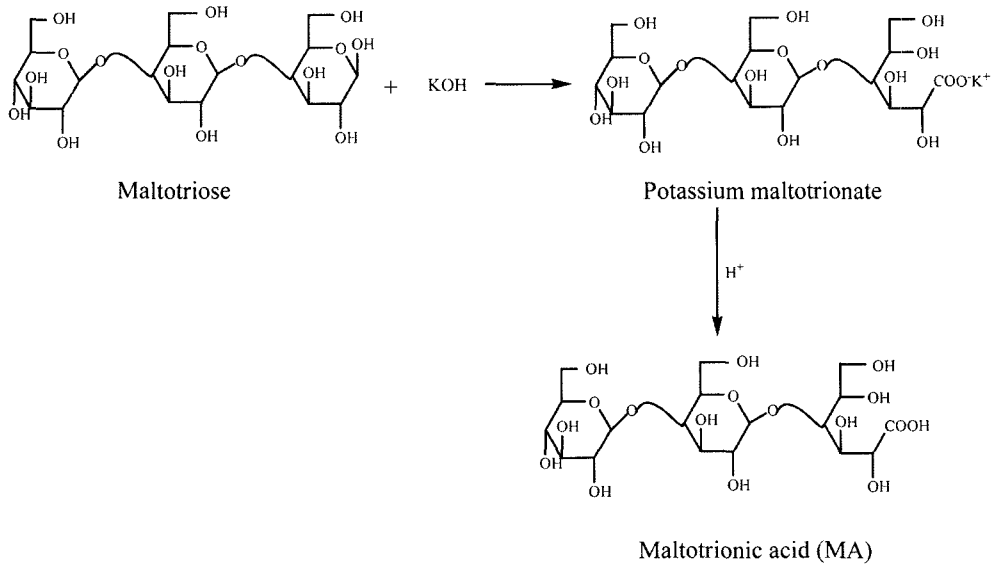

Figure 1. Schematic diagram showing the synthesis of maltotrionic acid (MA).

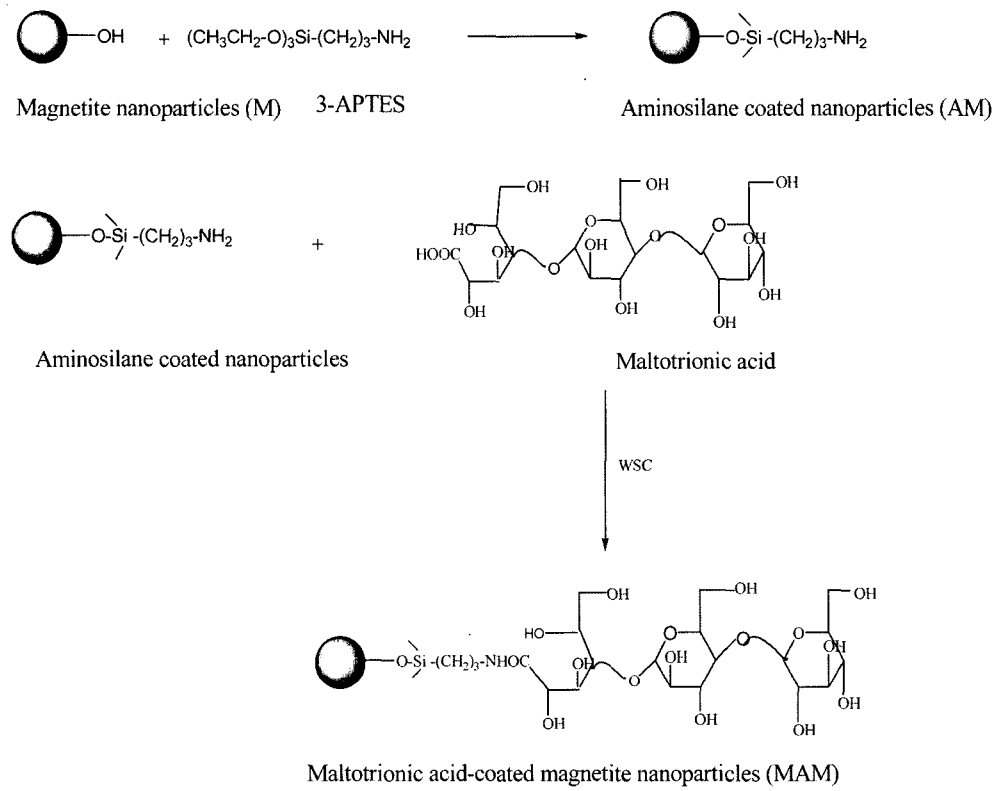

Figure 2. Synthesis of MA-grafted magnetite nanoparticles (MAM).

obtain MA-coated magnetite nanoparticles (MAM) (Figure 2).

Modification of MAM with FA: Firstly, MA-coated magnetite nanoparticles (MAM) were modified by silanization reaction as the procedure mentioned above (Figure 3). Then one gram of FA is dissolved in 50 mL dimethylsulfoxide (DMSO) and then dicyclohexylcarbodiimide (0.4754 g) and *N*-hydroxysuccinimide (NHS) (0.2652 g) are added to the solution. The solution is kept for one day for the activation of folate groups. After removing byproduct, dicyclohexylurea, by filtration, NHS-folate (50 mL) and MAM (5 mL)

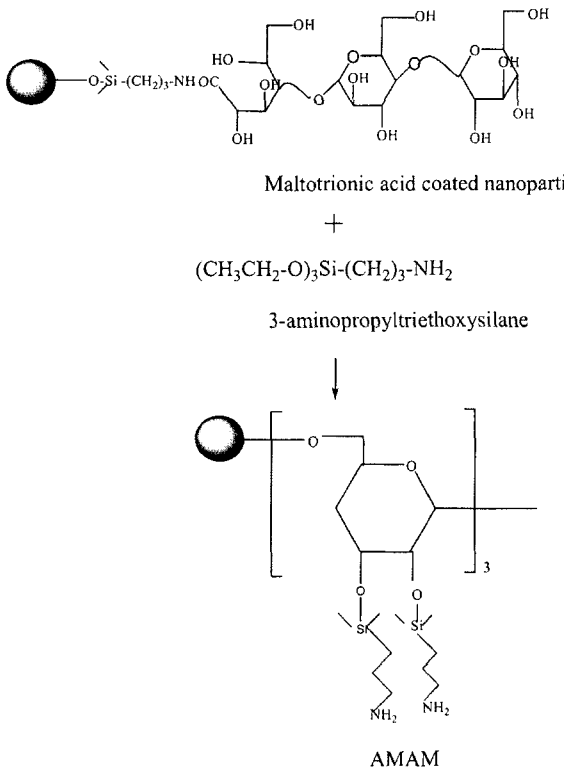

Figure 3. Modification of MAM with aminosilane (AMAM).

are mixed and taken in a round flask and the reaction mixture was stirred at about 150 rpm for 2 h. The reaction mixture was finally dialyzed against distilled water for 1 day.

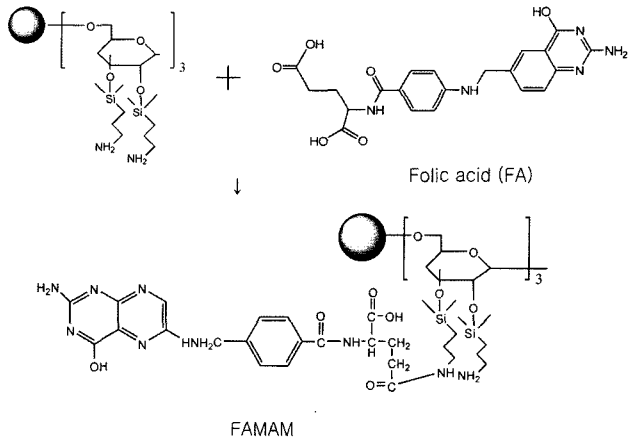

Figure 4. Modification of AMAM with FA (FAMAM).

Then the suspension was centrifuged and the precipitate i.e. MAM-folate (FAMAM) was washed with deionized water and subsequently vaccum-dried overnight (Figure 4).[21]

Modification of FAMAM with Fluorescein Isothiocyanate: The magnetite nanoparticles modified with FA (FAMAM) were used for further attachment of fluorescein isothiocyanate (FITC). The nanoparticles were added to the mixture of 4 mL of 0.015 M FITC solution in methanol, 1.5 mL of 15 mM *N*-hydroxysuccinimide (NHS) and 1.5 mL of 75 mM EDC solution in water, using triethylamine as a catalyst. The pH was adjusted to 9 and after incubation at 37 °C for 4 h, the mixture was centrifuged and the precipitate was washed by deionized water, and vacuum-dried overnight to get FITC-conjugated FAMAM (FFAMAM) (Figure 5).[12]

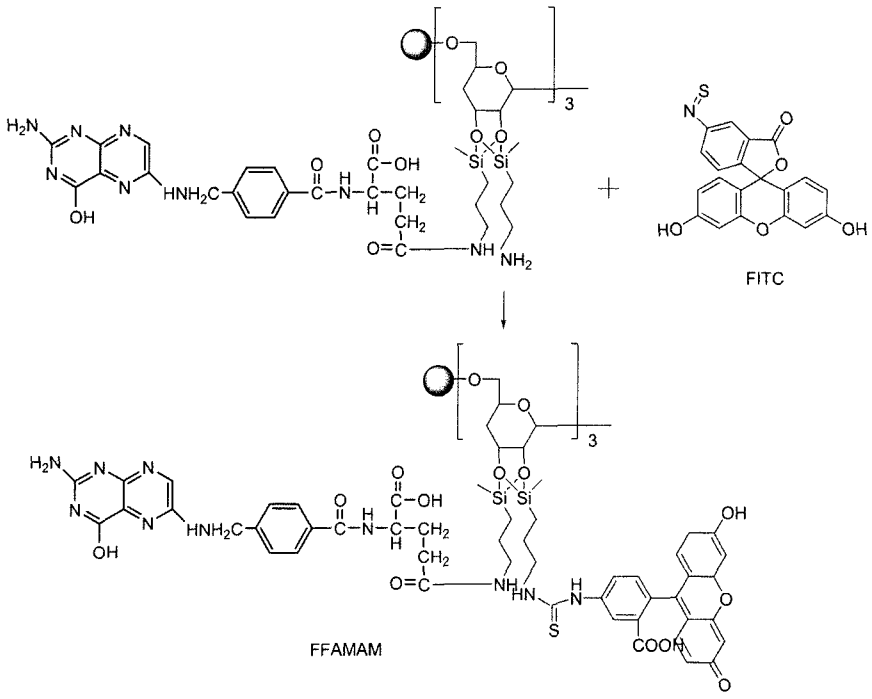

Figure 5. Modification of FAMAM with FITC (FFAMAM).

Characterization. Fourier transform infrared (FTIR) spectra were obtained using a Jasco, FTIR 300E spectrometer with a resolution of 4 cm^{-1}. To characterize the self-assembled monolayers formed on the surface of the nanoparticles, a small amount of nanoparticle powder was milled with KBr, and the mixture was pressed into a disc for analysis.

The transmission electron microphotographs (PHILIPS, CM 200 TEM, applied operation voltage, 120 kv) was used to observe the morphology of MAM. To obtain the samples for TEM observations, MAM were diluted with distilled water and then deposited on copper grid. After drying the magnetite fluids thin films on the copper grid, a thin layer of carbon films of about 10-30 nm in thickness was deposited on the magnetic fluids film.

The hydrodynamic diameter and size distribution of MAM were determined by DLS. A standard laboratory-built light scattering spectrometer using a BI 90 particle sizer (Brookhaven Instruments Corp., Holtsville, NY) with vertically polarized incident light of 514.5 nm supplied by an argon ion laser (Lexel laser, model 95) was used. The beam was focused onto the sample through a temperature-controlled chamber (temperature 25 °C, scattering angle 90°) filled with refractive index matching silicon oil. The sample solutions were filtered by 0.8 μm filter directly to preclean 10 nm NMR tubes.

A vibrating sample magnetometer (Digital measurement system, Inc. model 155) was employed to measure the magnetization of MAM at room temperature. To investigate the crystal structure of magnetite, X-ray diffraction (XRD, Enraf Nonius, RA/FR-571) was used.

Fluorescence and topographic images of cells were obtained with a combined explorer system with a motorized inverted fluorescence microscope, Leica DMIRB.

Three-dimensional image reconstructions of fluorescein-labeled nanoparticles were obtained with a Zeiss LSM 410 confocal laser scanning microscope (Zeiss, Oberkochen, Germany) equipped with a computer-controlled and motorized scan stage. An argon laser for FITC excitation at 488 nm was used for imaging. A 510-525 nm band-pass filter for the FITC emission signal was placed in the front of detectors.

Cell Culture. Human breast cancer cells (KB cells) were used in this experiment. Cells were routinely cultured at 37 °C in a humidified atmosphere with 5% CO_2 (in air), in a flask containing 10 mL of RPMI-1640 medium, supplemented with 10% fetal bovine serum (FBS) and 1% penicillin streptomicin G sodium (PGS). Media was changed every third day. For subculture, the cells were washed twice with PBS and incubated with trypsin-EDTA solution (0.25% trypsin, 1 mm EDTA) for 10 min at 37 °C to detach the cells, and the media were then added in the flask at room temperature to inhibit the effect of trypsin. The cells were washed twice by centrifugation and resuspended in the media to culture the cells in the new culture flasks. Cell viability was determined through staining with trypan blue and cells were counted using a hemocytometer. Cell density was estimated using a 0.9 mm^3 counting chamber.

To study cellular uptake of nanoparticles via fluorescence and confocal microscopy, FAMAM and FFAMAM were added to the cell culture media at a particle concentration of 0.2 mg/mL. The cells were cultured in 24-well plastic dishes for 20 h and then reseeded with the nanoparticle-dispersed culture media. After 48 h of incubation at 37 °C, the cells were washed twice with PBS and fluorescence and confocal microscopy images of the cells were taken.

Results and Discussion

Surface Characterization. To confirm the presence of crystalline magnetite within the polymer particles, the structure of the magnetic polymer particles was characterized by XRD and the diffractogram is shown in Figure 6. The position and relative intensity of the diffraction pattern of the MAM synthesized in this study are close to the standard pattern for crystalline magnetite with spinel structure, which has six diffraction peaks : {220}, {311}, {400}, {422}, {511} and {440}.[22] It is clearly seen that the particles did not show sharp diffraction peaks but show a broadband. This is typical for amorphous materials and also for ultrafine crystalline materials in which diffraction peaks can not be well resolved. Therefore, it could be concluded that the iron oxide species present in the polysaccharide particles were the desired Fe_3O_4 with spinel structure.

TEM was used to characterize the morphology and size of MAM in the solid state. Figure 7 shows that the particles are shaped spherically and monodispersed with an average size of 7 nm. The electron diffraction pattern shown in Figure 7(a) which consists of rings, was consistent with a cubic inverse spinel structure of MAM, indicating the good crystallinity of the magnetite nanoparticles. The characteristic d spacing corresponds to the hkl value {220}, {311}, {400},

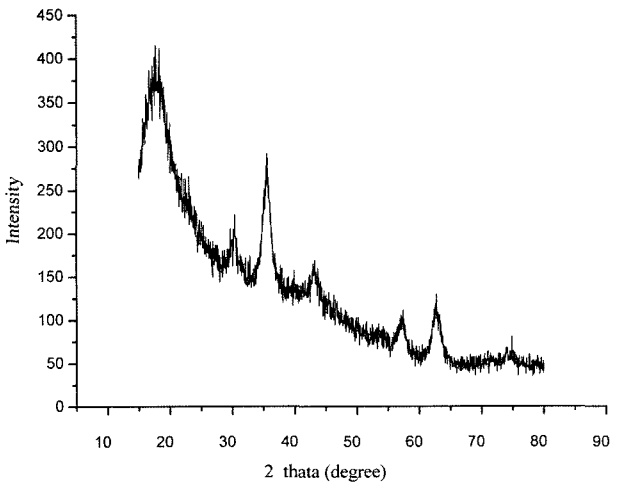

Figure 6. XRD pattern of MAM.

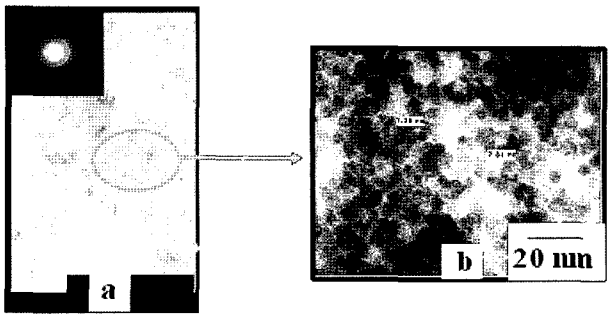

Figure 7. TEM images of MAM.

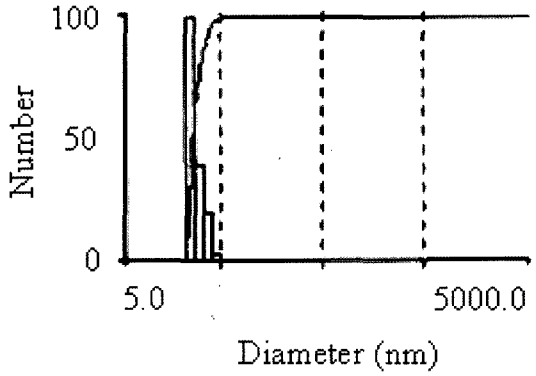

Figure 8. Particle size distribution of MAM by DLS.

{440}, {533}, suggesting a very good coincidence with the XRD data.[23]

Figure 8 shows the typical size and size distribution of synthesized MAM measured by DLS. It can be seen from the figure that MAM display an unimodal size distribution and the average hydrodynamic diameter of the coated magnetite was about 26 nm (data not shown). The size as determined by DLS was larger than that determined by TEM as expected. This is because DLS technique gives a mean hydrodynamic diameter of the magnetite core surrounded by the organic and solvation layers whereas TEM gives the diameter of the core alone.

To determine the magnetic properties of MAM, a vibrating sample magnetometer (VSM) was used. Figure 9 shows magnetization of MAM at room temperature. It shows no hysteresis loops and the magnetization curve exhibits zero remanence and coercivity, which proves that magnetite nanoparticles have superparamagnetic properties and they are single-domain nanoparticles.[24] The superparamagnetism enables the nanoparticles to respond to an applied magnetic field without any permanent magnetization and redisperse rapidly when the magnetic field is removed. The saturation magnetization of the obtained MAM was 23 emu/g. This large saturation magnetization of magnetite nanoparticles makes them very susceptible to magnetic fields, and therefore makes the solid and liquid phase separate easily.

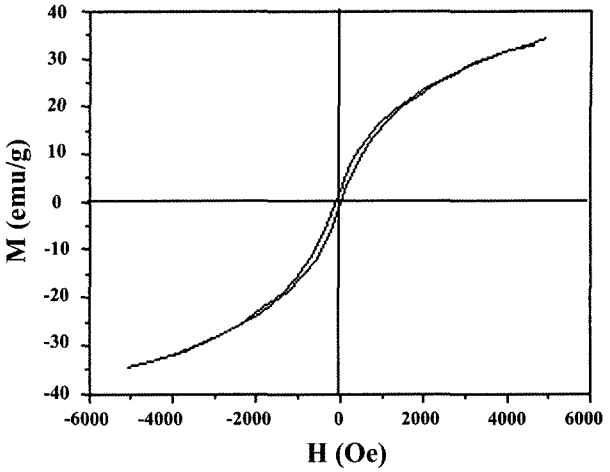

Figure 9. Magnetization curve of MAM obtained by VSM.

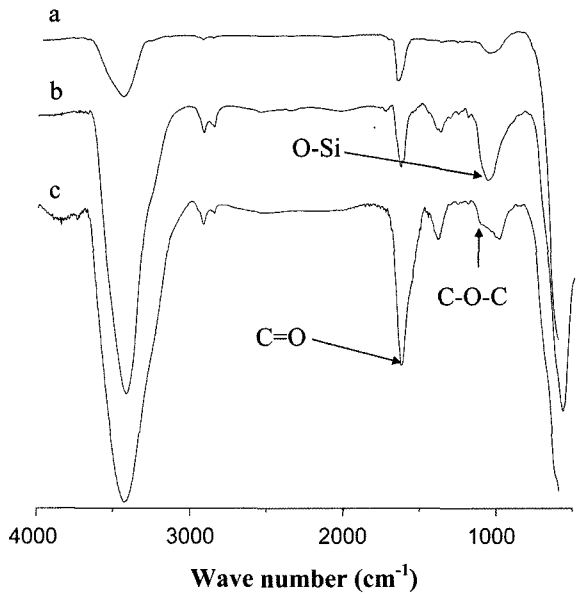

Figure 10. FTIR spectra of MAM (a), AMAM (b) and FAMAM (c).

The surface modification of magnetite nanoparticles with MA and FA was confirmed by FTIR, as displayed in Figure 10. The band near to 1108 cm^{-1} is ascribed to the vibration of the C-O at the C-4 position of glucose residue.[25] Again, MA represents typical absorption of 3450 and 1740 cm^{-1} which correspond to hydroxyl (-OH) and carboxylic acid (-COOH), respectively, are also shown in Figure 10(a), indicating the introduction of MA on the surface of magnetite. The introduction of silane to the surface of MAM was confirmed by the bands at 1113 and 1048 cm^{-1} assigned to the O-Si groups.[26] The two broad bands at 3417 and 1625 cm^{-1} can be ascribed to the N-H stretching vibration and NH_2 bending mode of free NH_2 groups, respectively. The FTIR spectrum of

FAMAM are shown in Figure 10(c). After modification with FA absorption peak at around 1600 cm^{-1} increased greatly without showing extra any other peak, suggesting that folate group was attached on the MAM. This is because FA itself contains amide bonds. The increase and broadening of amide bands in the FTIR spectrum of MAM can be attributed to linkage between MA and FA via an amide bond.

Cell Culture. Figure 11 shows the phase contrast photographs ($\times$ 200) of KB cells (a), after 48 h culture in a media containing MAM (b) and FAMAM (c). The incubation of the cells with MAM and FAMAM did not alter the morphology of cell types. The morphology of the cells after 48 h incubation with MAM and FAMAM (Figures 11(b) and 11(c), respectively) were close to that of the control cells (Figure 11(a)), suggesting the biocompatibility of the modified magnetite nanoparticles.

The uptake of FITC-MAM and FFAMAM was visualized using fluorescence microscopy. Figure 12 shows fluorescence images of KB cells after culture in a media containing FITC-MAM (Figure 12(a)) and FFAMAM (Figure 12(b)). Fluorescence corresponded with the exact location of the cells. A significant uptake of nanoparticles was clearly observed from the fluorescence images, suggesting that the nanoparticles were internalized in the cells. Furthermore, it was observed that the amount of uptake of FFAMAM into cells was higher than that of FITC-MAM. This result indicates that FA modification not only facilitated the nanoparticles to target specific cells, but also increased the yield of cell internalization. The interaction between FA and folate receptors expressed on the membrane surface of cancer cells might have contributed to the improvement of nanoparticles uptake, based on receptor mediated endocytosis.[22]

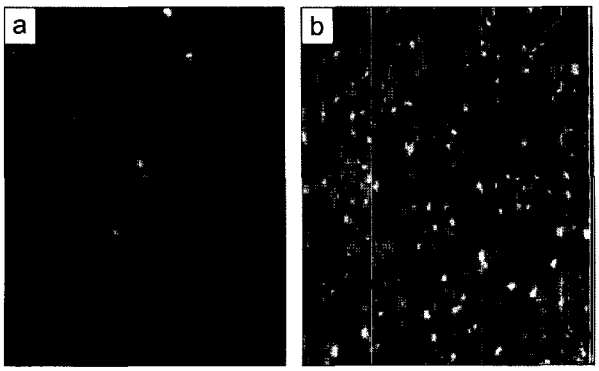

Figure 12. Fluorescence microscope images of KB cell in the presence of FITC-MAM (a) and FFAMAM (b).

The internalization of FFAMAM into KB cells was also confirmed by confocal microscopy performed at various depth of cell surface, showing weak signal at top (Figure

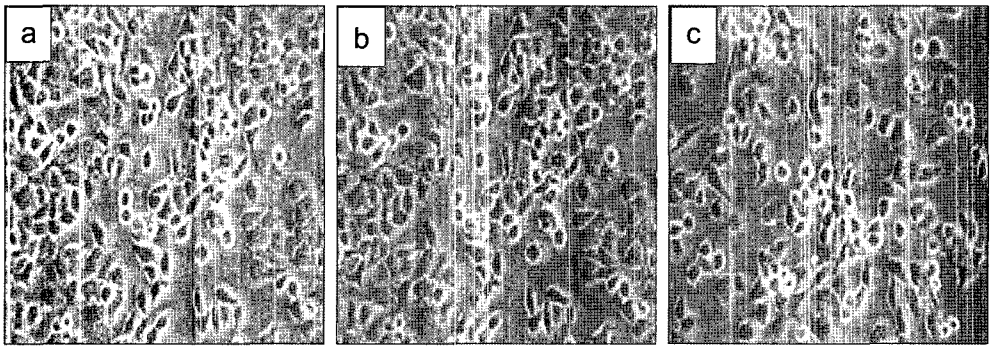

Figure 11. Phase contrast photographs of KB cell (a), after 48 h culture in a media containing MAM (b), and FAMAM (c).

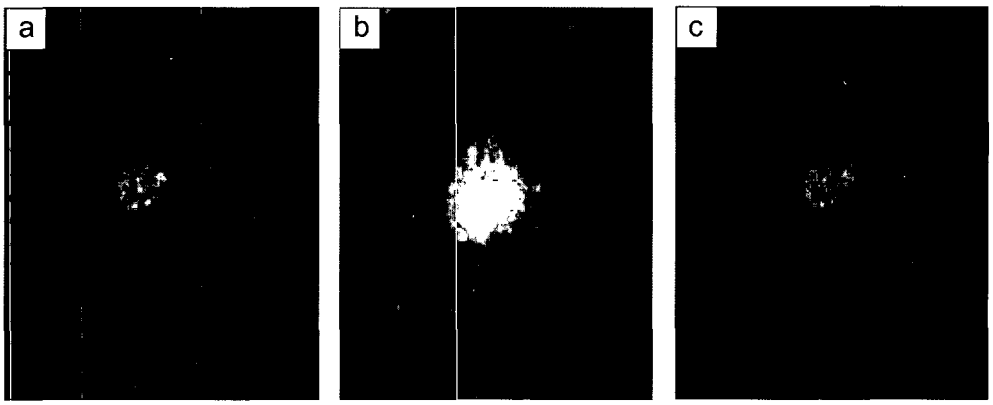

Figure 13. Confocal microscope images of KB cells cultured in the presence of FFAMAM : top (a), middle (b), and bottom (c) of the cells.

13(a)) and the bottom (Figure 13(c)) of the cells but intense signal in the middle (Figure 13(b)). The results suggested that many nanoparticles are internalized in the cytoplasm i.e. the fluorescence signal originates from the cell interior. Because the nanoparticles are rather small, receptor-mediated endocytosis is a likely mechanism for internalization.

Conclusions

In this study, superparamagnetic magnetite nanoparticles with size approximately 7 nm were successfully modified using MA and FA, and characterized by various physicochemical means. The colloidal solution of nanoparticles showed high stability and monodispersity after MA immobilization as determined by TEM and DLS. The results of cell culture experiment indicated that MAM and FAMAM were biocompatible. The fluorescence and confocal microscope results showed that the nanoparticles modified with MA and FA were internalized into breast cancer cell (KB cells). The amount of uptake of FAMAM was much higher than that of MAM. This result suggests that the modification of magnetite nanoparticles with both MA and FA could be used to facilitate the nanoparticle uptake to specific KB cells for molecular imaging.

Acknowledgements. This work was supported by a grant from The Advanced Medical Technology Cluster for Diagnosis and Prediction at KNU from MOCIE, The Republic of Korea.

References

(1) A. Halbreich, J. Roger, J. N. Pons, M. F. Da Silva, E Hasmonay, M. Roudier, M. Boynard, C. Sestier, A. Amri, D. Geldwerth, B. Fertil, J. C. Bacri, and D. Sabolovic, in *Scientific and Clinical Applications of Magnetic Carriers*, U. Hafeli, W. Schutt, J. Teller, and M. Zborowski, Eds., Plenum Press, New York, 1997, pp 399-417.
(2) A. Halbreich, J. Roger, J. N. Pons, D. Geldwerth, M. F. Da Silva, M. Roudier, and J. C. Bacri, *Biochimie*, **80**, 379 (1998).
(3) L. A. Perrin-Cocon, P. N. Marche, and C. L. Villiers, *Biochem. J.*, **338**, 123 (1999).
(4) S. H. Koenig and K. E. Kellar, *Acad. Radiol.*, **3**, 273 (1996).
(5) N. Kohler, C. Sun, J. Wang, and M. Zhang, *Langmuir*, **21**, 8858 (2005).
(6) J. Roger, J. N. Pons, R. Massart, A. Halbreich, and J. C. Bacri, *Eur. Phys. J. Appl. Phys.*, **5**, 321 (1999).
(7) P. Moroz, S. K. Jones, and B. N. Gray, *Int. J. Hyperthermia*, **18**, 267 (2002).
(8) F. Bertorelle, C. Wilhelm, J. Roger, F. Gazeau, C. Menager, and V. Cabuil, *Langmuir*, **22**, 5385 (2006).
(9) Y. Zhang and J. Zhang, *J. Colloid Interface Sci.*, **283**, 352 (2005).
(10) N. Sadeghiani, L. S. Barbosa, L. P. Silva, R. B. Azevedo, P. C. Morais, and Z. G. M. Lacava, *J. Magn. Magn. Mater.*, **289**, 466 (2005).
(11) A. K. Gupta and M. Gupta, *Biomaterials*, **26**, 1565 (2005).
(12) Y. Zhang, N. Kohler, and M. Zhang, *Biomaterials*, **23**, 1553 (2002).
(13) L. M. Lacava, Z. G. M. Lacava, M. F. Da Silva, O. Silva, S. B. Chaves, R. B. Azevedo, F. Pelegrini, C. Gansau, N. Buske, D. Sabolovic, and P. C. Morais, *Biophys. J.*, **80**, 2483 (2001).
(14) L. Babes, B. Denzoit, G. Tanguy, J. J. Le Jeune, and P. Jallet, *J. Colloid Interface Sci.*, **212**, 474 (1999).
(15) J. Dietvorst, J. Londesborough, and H. Y. Steensma, *Yeast*, **22**, 775 (2005).
(16) F. Bealin-Kelly, C. T. Kelly, and W. M. Fogarty, *Biochem. Enzymol.*, **1**, 149 (1990).
(17) M. Nakano, H. Chaen, T. Sugimoto, and T. Miyake, US Patent 5739024 (1998).
(18) S. D. Weitman, R. H. Lark, L. R. Coney, D. W. Fort, V. Frasca, V. R Zurawski, and B. A. Kamen, *Cancer Res.*, **52**, 3396 (1992).
(19) P. A. Dresco, V. S. Zaitsev, R. J. Gambino, and B. Chu, *Langmuir*, **15**, 1945 (1999).
(20) Y. K. Park, Y. H. Park, B. A. Shin, E. S. Choi, Y. R. Park, and T. Akaike, *J. Control. Release*, **69**, 97 (2000).
(21) H. Choi, S. R. Choi, R. Zhou, H. F. Kung, and I.-W. Chen, *Acad. Radiol.*, **11**, 996 (2004).
(22) X. Liu , H. Liu, J. Xing, Y. Guan, Z. Ma, G. Shan, and C. Yang, *Chaina Particuology*, **2**, 76 (2003).
(23) A. Guinier, *X-ray diffraction in crystals, imperfect crystals, and amorphous bodies*, Sanfrancisco, Freeman, 1963, p. 378.
(24) M. A. Zhiya, G. Yueping, and H. Liu, *J. Polym. Sci., Polym. Chem.*, **43**, 3433 (2005).
(25) K. I. Shingel, *Carbohydr. Res.*, **337**, 1445 (2002).
(26) M. Yamaura, R. L. Camilo, L. C. Sampaio, M. A. Macedo, M. Nakamura, and H. E. Toma, *J. Magn. Magn. Mater.*, **279**, 210 (2004).